ELSEVIER

Biochimica et Biophysica Acta 1291 (1996) 35–39

BBA Biochimica et Biophysica Acta

Intranuclear distribution of 2,2′,4,4′,5,5′-hexachlorobiphenyl and 2,3,7,8,-tetrachlorodibenzo-*p*-dioxin

Eleonore Glitz, Klaus Buff *

Abteilung für Zellchemie, GSF-Forschungszentrum für Umwelt und Gesundheit Neuherberg, Postfach 1129, D-85758 Oberschleißheim, Germany

Received 27 November 1995; revised 22 March 1996; accepted 17 April 1996

Abstract

The in vitro intranuclear distribution of the chlorinated aromatic hydrocarbon compounds 2,2′,4,4′,5,5′-hexachlorobiphenyl and 2,3,7,8-tetrachlorodibenzo-*p*-dioxin was determined in isolated rat liver cell nuclei. Suspended nuclei were incubated with the ^{3}H-labeled congeners, and the incubation terminated by brief UV irradiation. High-intensity UV irradiation at 254 nm changes the reversible association between macromolecules and ligands into covalent linkages and thus stabilizes the equilibrium distribution. The nuclei were then fractionated with the radioactive congeners covalently linked to the purified fractions. The intranuclear distribution of the model compounds was not uniform. The majority of either chemical was attached to the nuclear envelope and to the chromatin fraction. Much lower amounts were bound to nucleoli. The nuclear matrix was almost devoid of the chemicals. Minute amounts of either compound were detected in association with DNA, none with nuclear RNA. The substantial association of these chlorinated hydrocarbon model compounds with chromatin may bear more general biological relevance and point to detrimental effects on the genetic apparatus. The presented method yields an unequivocal profile of the genuine nuclear distribution of photoactivatable chemicals.

Keywords: Dioxin; Nuclear distribution; Photo-induced binding; Polychlorobiphenyl; Tetrachlorodibenzo-*p*-dioxin

1. Introduction

Uptake of environmental pollutants by ingestion and inhalation provides for a steady supply of exogenous chemicals in mammals. All kinds of xenobiotics have been found in human tissues. In particular, polychlorinated biphenyls (PCB) and chlorinated dioxins may reach concentrations in human tissues that deserve concern on potential toxic effects.

The hub of cellular interaction of PCB and 2,3,7,8-tetrachlorodibenzo-*p*-dioxin (TCDD) with macromolecules is their highly specific and mutually competitive binding to the cellular Ah-receptor protein in the cytosol [1–3]. Apart from this receptor, a soluble PCB binding protein in rat liver cells has recently been uncovered [4] and enriched from rat liver cytosol [5]. It is a 40 kDa binding protein, specifically and with high affinity for the PCB congeners 2,2′,4,4′,5,5′-hexachlorobiphenyl and 3,3′,4,4′,5-pentachlorobiphenyl, but with low-affinity only for 3,3′,4,4′-tetrachlorobiphenyl [5]. The protein is localized in the cell cytosol but is absent in the cell nucleus [6]. Conversely, analysis of nuclear DNA adducts, ^{32}P-postlabeled after photo-induced covalent binding of 2,2′,4,4′,5,5′-hexachlorobiphenyl in cultured human cells, has revealed that PCB congeners distribute also into cell nuclei [7].

We studied the nuclear whereabouts of these chemicals after in vitro uptake in some detail. Basically, the intranuclear equilibrium distribution of the two compounds was looked for, irrespective of the presence of potential specific binding proteins in the cell cytosol.

The experimental method of choice was, first, to equilibrate the isolated nuclei with the radioactive (^{3}H-labeled) chemicals and, then, to stabilize the equilibrium distribution by brief high-intensity UV irradiation. It has previously been shown that excited intermediates of photoactivatable ligands can react with their nearest neighbours by generating covalent bonds by 'freezing' the equilibrium distribution of ^{3}H-labeled chemicals such as 2,2′,4,4′,5,5′-hexachlorobiphenyl (6-CB) [7,8]. Since weak and strong associations will be affected alike, the experimental conditions used do not demand for discrimination of 'specific' from 'non-specific' binding sites: the labeled binding sites

Abbreviations: PCB, polychlorinated biphenyls; 6-CB, ^{3}H-labeled 2,2′,4,4′,5,5′-hexachlorobiphenyl; TCDD, ^{3}H-labeled 2,3,7,8-tetrachlorodibenzo-*p*-dioxin.

* Corresponding author. Fax: +49 89 31873322.

PII S0304-4165(96)00041-4

in total will mirror the original distribution. The nuclei were, lastly, fractionated and subnuclear fractions isolated with the radioactive compounds covalently bound to their original targets. The measured radioactivity of the purified fractions gives then the relative distribution in terms of protein binding. By taking the volume ratios of the nuclear components into account, the relative intranuclear distribution in terms of concentration could be computed. Experiments in the absence of UV irradiation showed low binding of radioactivity only or even no radioactivity at all, due to considerable loss of bound ligands during fractionation of nuclei.

The in vitro approach offers a useful tool to track the nuclear distribution and potential macromolecular targets of photoactivatable lipophilic chemicals.

2. Materials and methods

2.1. Chemicals

^{3}H-labelled 2,2′,4,4′,5,5′-hexachlorobiphenyl (0.3 TBq/mmol = 8 Ci/mmol) was synthesized as described [4]. 2,3,7,8-tetrachloro-[^{3}H]dibenzo-*p*-dioxin (1.5 TBq = 40 Ci/mmol) was kindly donated by Dr. P. Cikryt (Universität Würzburg, Germany). Batches of either radiochemical were monthly purified by TLC (in n-hexane on silica gel plates), the radiochemical purity of the scraped-off material being > 95%. Fine chemicals were purchased from Fluka (Neu-Ulm, Germany) and Merck (Darmstadt, Germany), enzymes were bought from Sigma (Deisenhofen, Germany), respectively.

2.2. Animals

Approx. 8 week-old Sprague–Dawley rats were housed in the GSF animal station. Ether-anesthesized animals, irrespective of sex, were used for liver excision. Tissue homogenization and all preparative steps of nuclear fractionation were performed at 0°C–4°C.

2.3. Isolation of rat liver nuclei [9]

Liver tissue, pooled from five animals, was minced and homogenized with a motor-driven Teflon pestle in 60 ml of 10 mM potassium phosphate buffer (pH 7.5). The homogenate was centrifuged (830 × *g*, 10 min), and the pellet was washed twice with 0.24 M sucrose in Hepes buffer (10 mM Hepes, 5 mM $MgCl_2$, 1 mM EDTA, 1 mM dithiothreitol, 0.2 mM phenylmethylsulfonyl fluoride, 0.03 mM leupeptin, pH 7.8). The suspension was cleared through a nylon mesh and centrifuged (3000 × *g*, 10 min). The precipitate was taken in 80 ml of 0.24 M Hepes-buffered sucrose, mixed with 320 ml of 2.4 M Hepes-buffered sucrose and layered in 35 ml portions on top of 5 ml 2.2 M Hepes-buffered sucrose for centrifugation (100 000 *g*, 60 min). The pellet was washed in 0.25 M sucrose in Hepes buffer, collected by centrifugation and stored at −80°C in buffer (approximately 2 × 108 nuclei/ml buffer: 50 mM Tris acetate, 5 mM $MgCl_2$, 40% glycerol, 1 mM EDTA, pH 8.3). Purity and integrity of the nuclei were checked by light microscopy and transmission electron microscopy (courtesy of Dr. U. Heinzmann, GSF).

2.4. Incubation and photofixation

5×10^7 Nuclei/ml were incubated in Hepes buffer at 10 nM concentration of either compound at 20°C for 20 min. The samples were briefly UV-irradiated (Philips HPK

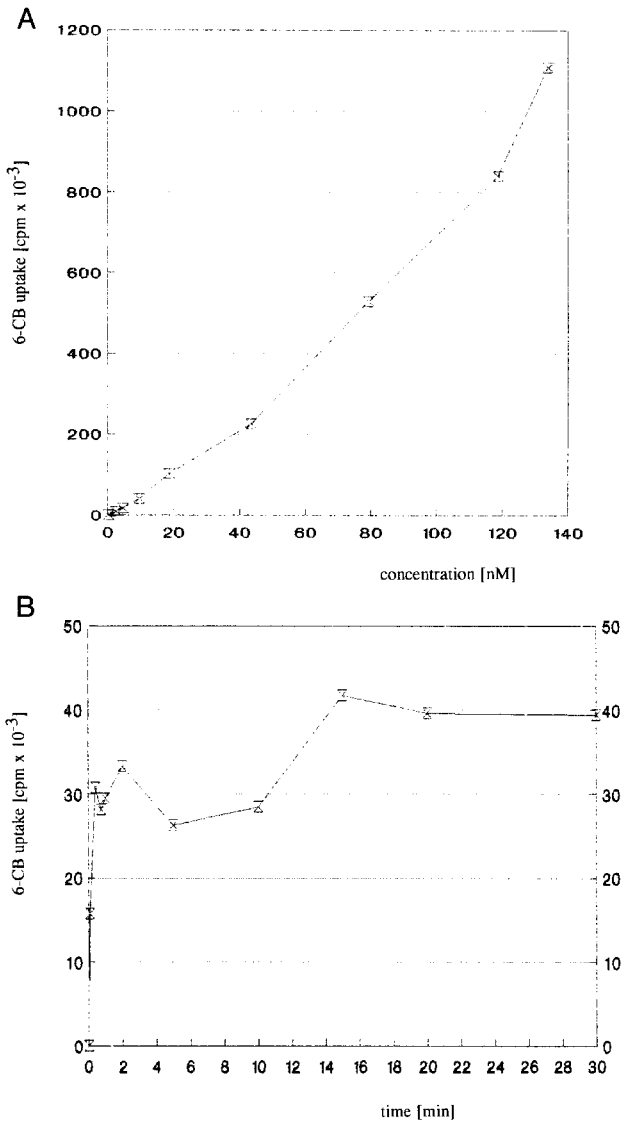

Fig. 1. Uptake of 6-CB by rat liver nuclei in suspension. Panel A: dependence on concentration. Nuclei were incubated for 25 min at the 6-CB concentrations indicated. Panel B: influence of incubation time. Nuclei were incubated with 10 nM = 55000 cpm of 6-CB for the time periods indicated. The results of one experiment are shown. Details are as in Section 2.

125-W/L mercury lamp, 254 nm, 25 sec, 2.5 cm distance; cf. Ref. [8]) to fix the chemicals covalently to their targets. The nuclei were collected (2500 × *g*, 10 min) and washed once with Hepes buffer. The yield of photo-induced 6-CB binding to cell fractions averaged 30%. The yield of TCDD photobinding was not determined due to sparing material; circumstantial evidence put the yield lower than that of 6-CB.

2.5. Fractionation of nuclei

After photofixation of the equilibrium distribution, the nuclei were fractionated according to established procedures. The preparative methods are summarized as follows: *nuclear envelope*: Riedel and Fasold [10]; Dwyer and Blobel [11]; *nuclear pore complex + lamina*: Dwyer and Blobel [11]; Bachs et al. [12]; *nuclear membrane*: Franke et al. [13]; *nucleoli*: Beebee [14]; *chromatin*: Addey and Campbell [15]; Johns [16]; *non-histone proteins*: Sanders [17]; Wilson and Spelsberg, 1975 [18]; *histone subfractions*: Johns [16]; *HMG proteins*: Sanders [17]. The purity of each fraction was checked by appropriate means, such as transmission and scanning electron microscopy (Dr. U. Heinzmann, GSF), chemical assays and SDS gel electrophoresis. The micrographs and the analytical results matched those known from textbooks and are, therefore, not repeated here.

2.6. Miscellaneous methods

DNA was isolated as described in the 'Maniatis Laboratory Manual' [19]; purity matched the published A_{260}-to-A_{280} ratio of 1.75–2.05. RNA was isolated by acid guanidiniumthiocyanate/phenol/chloroform extraction [20]. Protein was measured according to established methods [21,22]. Radioactivity of ^{3}H-labeled purified samples was measured by liquid scintillation counting (Packard TriCarb 300).

3. Results and discussion

Conditions of 6-CB and TCDD uptake by suspended nuclei were determined in pilot experiments. Uptake of 6-CB was linear up to 130 nM (Fig. 1A), equilibrium was approached after 15 min (Fig. 1B). Similar results were obtained with TCDD (data omitted). Uptake of the model compounds by suspended nuclei is thus not limited by saturation at the low concentrations of interest. The results of these pilot studies yielded the optimum incubation conditions for all the subsequent incubation assays prior to irradiation: an as low as possible 'physiological-like' concentration — i.e., 10 nM — with sufficient radioactivity — i.e., approx. 50 000 cpm/mg protein — and an incubation time to reach equilibrium; i.e., 20 min.

The results of the 6-CB and TCDD distribution in nuclear fractions are compiled in Table 1. Heavy radioactive labeling of protein is found in the nuclear envelope. The nuclear envelope is composed of two layers, the lipid-rich nuclear membrane and underneath the protein-rich pore complex + lamina. The rigorous purification employed [11–13] resulted in very low absolute amounts of labeling. The relative labeling ratio would indicate that the relative lipid-rich nuclear membrane of the composite is somewhat preferred over the lamina layer. Second to the envelope, protein-bound radioactivity is found in the nucleolus and in the chromatin fraction. Within the chromatin, the group of non-histone proteins is the major

Table 1
Binding of 6-CB and TCDD to protein of nuclear fractions

Nuclear fraction	6-CB bound (ng/mg) *	*n*	TCDD bound (ng/mg) *
Nuclear envelope	93.5 ± 15.5	3	6.2
Membrane	0.96 ± 0.5	3	0.5
Pore complex + lamina	0.35 ± 0.02	3	0.08
Nuclear extract	0.3 ± 0.06	3	0.04
Chromatin	4.1 ± 0.74	12	0.76
Histones	0.26 ± 0.06	4	0.02
H1	0	2	
Core	0.32 ± 0.1	2	
Non-histone protein	2.0 ± 0.35	5	0.82
High-mobility-group			
Protein	0	2	
Nucleolus	2.0 ± 0.2	4	0.92
DNA	0.004 ± 0.01	4	0.0055
Nuclear RNA	0	4	0

Cell nuclei in suspension were incubated (20 min, 20°C) with the chemical of choice (10 nM). The equilibrium distribution was fixed by irradiation. The nuclei were fractionated and bound radioactivity was determined as described in Section 2. 6-CB: the mean ± S.D. of *N* independent experiments is shown; TCDD: the mean ± 20% deviation of 2 independent experiments is shown. In the absence of UV irradiation, binding of 6-CB was 22 ng/mg protein to the nuclear envelope and 0 ng/mg DNA to DNA.

* mg protein or mg nucleic acid, respectively.

binding site. Analysis of histones (done only with 6-CB) reveals the core histones H2–H4 as major targets. There is a lack of association with the linker histone H1. This is remarkable in that models of chromatin show large parts of the linker histone H1 surface exposed to the nuclear matrix [23]. The proteins of the nuclear extract are poorly labeled; partly may be as a result of the in vitro conditions employed (absence of specific cellular binding proteins), but essentially due to the lack of lipid-rich structures in the nuclear matrix. There is also a complete lack of binding to the High Mobility Group proteins. Minute quantities of 6-CB and TCDD are associated with nuclear DNA, none with RNA. The throughout lower labeling efficiency of TCDD compared with 6-CB is very likely the result of photo-excited chemical intermediates with greater chemical stability.

Aside from protein binding, the distribution of exogenous chemicals can also be expressed in relation to concentration (volume). Using the binding data of Table 1, the data were calculated by accounting for the protein content and the volume ratios of the individual nuclear fractions. The distribution within volume was calculated on the following assumptions: (i) the protein content of chromatin, of the nucleolus, of the nuclear envelope and of the nuclear extract is 80%, 80%, 60% and 30%, respectively; (ii) their volume percentage is assumed as in the literature (cf. legend of Table 2); (iii) the yield of photobinding is similar for all fractions (based on a 30% yield in previous experiments; cf. Ref. [8]). Under these assumptions, the volume-related distribution, listed in Table 2, was obtained. The results confirm the nuclear envelope and chromatin as the prominent nuclear targets of 6-CB and TCDD, the nucleolus being a candidate target for TCDD. The nuclear matrix space is virtually devoid of the xenobiotics, minute concentrations are encountered in direct proximity of DNA. In a final step of transformation, the numerical data of Table 2 are visualized by the graphical illustration shown in Fig. 2. The plot presentation gives a lucid view of the strong enrichment of these lipophilic chemicals in the small volume of the nuclear envelope, in contrast to the virtually 'clean' nuclear matrix (nuclear extract). Since the plots mirror the relative equilibrium distribution at low non-saturating conditions, an apparent accumulation of dots does not necessarily indicate saturation phenomena.

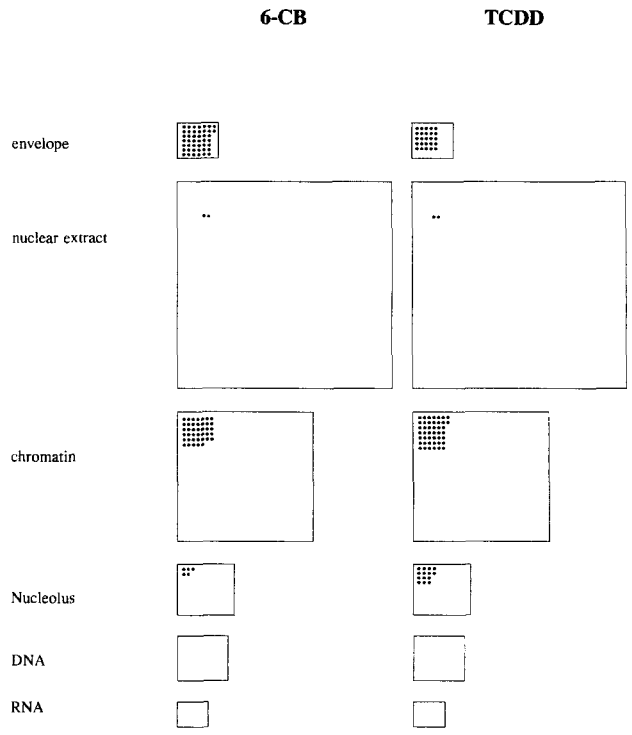

Fig. 2. Plot of the relative distribution of 6-CB and TCDD in nuclear fractions. The numerical data of Table 2 were transformed in a graphic plot to illustrate the relative distribution of 6-CB and TCDD in different volumes of nuclear compartments. The size of each square symbolizes in proportion (Table 2) the volume percentage of the respective nuclear fraction. The number of dots within each square stands for the relative concentration of the respective chemical in the individual nuclear fraction, one dot symbolizing 1% of total distribution.

In summary, the nuclear envelope represents the first defense line against intruding exogenous chemicals. However, once the chemicals overcome this barrier, they distribute widely into and throughout the interior of the nucleus. They associate preferentially with protein-dense

Table 2
Relative distribution of 6-CB and TCDD in nuclear fractions

Fraction	Volume * (% of nucleus)	Distribution (% of total compound)	
		6-CB	TCDD
Envelope	2	43.8 ± 9.2	25
Nuclear extract	65	2.2 ± 0.2	2.1
Chromatin	25	40.0 ± 5.7	44
Nucleolus	4	4.5 ± 0.5	14.6
DNA	3	< 0.01	0.3
Nuclear RNA	1	0	0

In order to indicate the relative concentration of either chemical in the nuclear fractions, the data of protein binding (Table 1) were calculated with respect to the fractional volumes. The distribution is shown as percentage of total binding in the individual fractions. The difference to 100% indicates binding to structures not characterized.

* The volume percentage of nuclear fractions is based on (i) David, H. (1977) Quantitative Ultrastructural Data of Animal and Human Cells, pp. 134–149, Gustav Fischer, Stuttgart [25]; (ii) Sitte, P. (1981) Allgemeine Mikromorphologie der Zelle, in Die Zelle. Struktur und Funktion (Metzner, H., ed.), 3rd Ed., Wissenschaftliche Verlagsgesellschaft, Stuttgart [26].

structures such as the chromatin. The binding to chromatin could interfere with function of chromatin proteins that in turn would entail detrimental effects with considerable biological relevance. Evidence of this pathway has recently been presented: a potential of adverse effects was recognized in the interference of PCB with DNA transcription of oncogenes [24]. In general, the method presented could be useful in tracking intracellular distribution kinetics of of chemically stabile but photo-excitable organic chemicals, irrespective of the presence of specific high-affinity low-capacity binding sites, and in clarifying sites and capacity of nuclear constituents. The method thus also greatly enhances confidence in predicting biological targets of chemical pollutants that even may have as yet not recognized.

Acknowledgements

We are indebted to Dr. U. Heinzmann, 'Institut für Pathologie' at the GSF, for purity assessment of nuclear fractions by means of transmission and scanning electron microscopy. We like to thank Prof. J. Berndt, then head of the 'Abteilung für Zellchemie', for his continuous support and encouragement, and Mrs. A. Bründl for her expert technical assistance.

References

[1] Bandiera, S., Safe, S. and Okey, A.B. (1982) Chem. Biol. Interact. 39, 259–277.
[2] Safe, S., Bandiera, S., Sawyer, T., Zmudska, B., Mason, G., Romkes, M., Denomme, M.A., Sparling, J., Okey, A.B. and Fujita, T. (1985) Environ. Health Perspect. 60, 57–68.
[3] Van den Berg, M., De Jongh, J., Poiger, H. and J.R. Olson (1994) Crit. Rev. Toxicol. 24, 1–74.
[4] Buff, K. and Bründl, A. (1992) Biochem. Pharmacol. 43, 965–970.
[5] Bründl, A. and Buff, K. (1993) Biochem. Pharmacol. 45, 885–891.
[6] Schmitz, E., Buff, K. and Berndt, J. (1991) Biol. Chem. Hoppe-Seyler 372, 748–749.
[7] Buff, K., Wegenke, M. and Bründl, A. (1989) Biochem. Pharmacol. 38, 2773–2779.
[8] Bründl, A. and Buff, K. (1988) Biochem. Pharmacol. 37, 1601–1608.
[9] Blobel, G. and Potter, V.R. (1966) Science 154, 1662–1665.
[10] Riedel, N. and Fasold, H. (1987) Biochem. J. 241, 203–212.
[11] Dwyer, N. and Blobel, G. (1976) J. Cell. Biol. 70, 581–591.
[12] Bachs, O., Lanini, L., Seratosa, J., Coll, M.J., Bastos, R., Aligué, R., Rius, E. and Carafoli E., (1990) J. Biol. Chem. 265, 18595–18600.
[13] Franke, W.W., Keenan, T.W., Stadler, J., Genz, R., Jarasch, E.D. and Kartenbeck J. (1976) Cytobiologie 13, 28–56.
[14] Beebee, T.J.C. (1978) Biochem. J. 176, 715–725.
[15] Addey, C.V.P. and Campbell, A.M. (1986) in Nuclear Structures. Isolation and Characterization (MacGillivray, A.J. and Birnie, G.D., eds.), pp. 86–99, Butterworths, London.
[16] Johns, E.W. (1963) Biochem. J. 92, 55–59.
[17] Sanders, C. (1977) Biochem. Biophys. Res. Commun. 78, 1034–1042.
[18] Wilson, E.M. and Spelsberg, T.C. (1975) in Methods in Enzymology (O'Malley, B.W. and Hardman, J.G., eds.), Vol. 40, pp. 171–176, Academic Press, New York, NY.
[19] Sambrook, J., Fritsch, E.F. and Maniatis, T. (1989) Molecular Cloning, 2nd Ed., Vol. 3, Appendix, pp. E3–E5, E12, Cold Spring Harbor Press, Cold Spring Harbor, NY.
[20] Chomczynski, B. and Sacchi, N. (1976) Anal. Biochem. 72, 248–254.
[21] Bradford, M.M. (1976) Anal. Biochem. 72, 248–254.
[22] Lowry, O.H., Rosenbrough, N.J., Farr, A.L. and Randall, R.J. (1951) J. Biol. Chem. 193, 265–275.
[23] Alberts, B., Bray, D., Lewis, J., Raff, M., Roberts, K. and Watson, J.D. (1989) Molecular Biology of the Cell, 2nd Ed., 499 pp., Garland, New York.
[24] Jenke, H.S., Michel, G., Hornhardt, S. and Berndt, J. (1991) Xenobiotika 21, 945–960.
[25] David, H. (1977) Quantitative Ultrastructural Data of Animal and Human Cells, pp. 134–149. Gustav Fischer, Stuttgart.
[26] Sitte, P. (1981) Allgemeine Mikromorphologie der Zelle. in Die Zelle. Struktur und Funktion (Metzner, H., ed.), 3rd Ed., Wissenschaftliche Verlagsgesellschaft, Stuttgart.